Asymptotic analysis of self-excited and forced vibrations of a self-regulating pressure control valve

Simon Schröders · **Alexander Fidlin**

Abstract Pressure vibrations in hydraulic systems are a widespread problem and can be caused by external excitation or self-exciting mechanisms. Although vibrations cannot be completely avoided in most cases, at least their frequencies must be known in order to prevent resonant excitation of adjacent components. While external excitation frequencies are known in most cases, the estimation of self-excited vibration amplitudes and frequencies is often difficult. Usually, numerical studies have to be executed in order to elaborate parameter influences, which is computationally expensive. The same holds true for the prediction of forced oscillation amplitudes. This contribution proposes asymptotic approximations of forced and self-excited oscillations in a simple hydraulic circuit consisting of a pump, an ideal consumer and a pressure control valve. Two excitation mechanisms of practical interest, namely pump pulsations (forced vibrations) and valve instability (self-excited vibrations), are analyzed. The system dynamics are described by a singularly perturbed third-order differential equation. By separating slow and fast variables in the system without external excitation, a first-order approximation of the slow manifold is computed. The flow on the slow manifold is approximated by an averaging procedure, whose piecewise defined zero-order solution maps the valve's switching property. A modification of the procedure allows for the asymptotic approximation of the system's forced response to an external excitation. The approximate solutions are validated within a realistic parameter range by comparison with numerical solutions of the full system equations.

1 Introduction

Hydraulic pressure control valves are widely used in hydraulic transmission systems. Their application represents the simplest way of maintaining a desired pressure level within a certain part of the overall hydraulic circuit independently of the current power demand of the consumer. This is a standard feature of many hydraulic circuits and enables to feed several consumers out of one sub-circuit at the same time. These circuits are also called constant-pressure systems.

Pressure control valves can be designed both as poppet valves or as spool valves. The pressure regulation is realized via an internal pressure feedback to a control surface of the valve piston, providing a feedback force proportional to the system pressure. On the other hand, the piston movement changes a variable control gap, leading to a piston position dependent oil flow out of the system. The pressure level is adjusted by

S. Schröders (✉) · A. Fidlin
Institute of Engineering Mechanics, Karlsruhe Institute of
Technology (KIT), Kaiserstr. 10, 76131 Karlsruhe,
Germany
Email: simon.schroeders@kit.edu

applying a control force on the piston, acting against the pressure feedback force. This force can either be mechanic (typical for pressure relief valves or pressure reducing valves), hydraulic (pilot-operated pressure control valve) or magnetic (proportional valve). While the first variant merely enables one individual unchangeable set-pressure level, the other two valve types, capable of providing a variable control force, allow for more advanced applications, for example, in electro-hydraulic (e.g., brake- or clutch-) actuation mechanisms. From the above elucidations, it follows that pressure control valves are closed-loop control systems [18]. It can even be shown that the included pressure feedback has certain optimality properties in the sense of linear quadratic regulation problems [11]. However, like many closed-loop control systems, it is long known that pressure control valves exhibit stability problems.

Early discussions addressing instability phenomena in hydraulic control valve circuits have been published in the 1960s. In [7], the interaction between pipeline dynamics and valve piston is identified as a possible source of instability. In [19], the internal pressure feedback loop is detected to possibly destabilize the valve's equilibrium position and qualitative design recommendations are given to ensure stable operation conditions. A review of these and other early studies can be found in [8]. Recent investigations on local stability of pressure control valves are carried out analytically in [12,13,16] and experimentally in [1]. It is unanimously discovered that, e.g., high system damping or supply volume flow into the system stabilizes the valve, in case of both poppet and spool valves. Furthermore, local stability strongly depends on the valve's flow characteristic and hence on control edge geometry and leakage behavior.

Since these are purely local properties and given that nearly all hydraulic systems are inherently nonlinear, the question arises to what extent the investigation of local stability is capable of drawing conclusions about the valves suitability in practical use. In this context, two main questions arise: The first one is about the structure of the phase space, namely whether unstable limit cycles exist, which limit the domain of attraction of stable equilibrium positions. The second question is about the size of oscillation amplitudes and frequencies in case of an unstable equilibrium position. If the amplitudes remain small, it may be acceptable in some practical applications that the stability border is exceeded from time to time; however, in order to avoid

resonant interactions with other vibratory elements, the frequency has to be known, too. These questions have been firstly addressed in [13], where simple analytical conditions for global stability in the presence of linear viscous damping are derived. For the case of Coulomb friction and quadratic damping, a harmonic balance approach is applied to show that an unstable limit cycle exists around a stable equilibrium position, limiting the domain of attraction of stable solutions. Nevertheless, this investigations remain in some sense local, as they do not take the valve's switching property into account.

Since their impact vibrations promise the more interesting dynamical behavior, poppet valves have so far received most attention in the field of self-excited and forced vibration dynamical analysis. Numerical investigations of circuits involving poppet valves, disclosing non-smooth bifurcation scenarios and even chaotic solutions, can be found in [2,3,9,10,16]. The self-excited and forced oscillations of systems involving spool valves are numerically analyzed in [12,26,27].

Despite the efforts already made, a systematic investigation (either numerically or analytically) of pressure control valve dynamics is still pending. One reason may be that even the simplest circuits include a large quantity of parameters, rendering numerical investigations extremely complex and time consuming. Therefore, in order to gain a better understanding of the dynamical behavior, it would be helpful to complement these numerical investigations by analytical studies. To conduct these, knowledge of characteristic quantities (length, time, pressure) is essential, in order to properly scale system parameters and variables [17]. The hybrid nature of every hydraulic circuit (meaning that two physical domains are included) renders the search for these characteristic quantities very counterintuitive. For example, the undamped eigenfrequency of the mechanical part (valve piston) is often taken to compute a characteristic time scale, but, as will be shown later, has generally little to do with the valve's natural frequency inside a hydraulic circuit.

Among the first attempts to investigate nonlinear valve dynamics analytically, in [23] the method of multiple scales is exploited to analyze the nonlinear response of a relief valve with cubic spring stiffness under harmonic excitation. This analysis is built upon in [20], where saddle node bifurcations of the steady-state solutions are observed. However, the model, on which the investigations are founded, does not include

the aforementioned closed-loop property. Considering hydraulic servo-systems, singular perturbation techniques are exploited for the dynamical analysis and control design in [21,22,25]. In [18], an approach using singular perturbation and averaging technique is proposed to obtain a reduced-order model for an electro-hydraulic gearbox actuator featuring a hydraulic pressure control valve. The frequency of a dithering signal introduces the slow time scale, and it is observed that the dynamics of the pressure control sensing chamber and pipeline resonances are much faster compared to valve piston and line pressure dynamics. The reduced-order model is constructed by omitting the fast variables. Subsequently, the slow motion is averaged in order to obtain an autonomous system. In [16], a minimal model of a pressure control poppet valve is analyzed. By simplification of the equilibrium position, an analytical approximation of the stability border, on which a Hopf bifurcation occurs, is computed. Furthermore, by means of a center manifold reduction, analytical approximations for the amplitude and frequency of the arising limit cycle oscillations are found, which, however, are very rough and which do not account for impacting solutions. The method of direct separation of motion is proposed in [14,15] to compute the effect of high-frequency excitation in form of a dithering signal on the stationary operating point of a pressure control valve with linear and quadratic damping.

Most of these studies have in common that an external frequency (corresponding to a dither signal or to a control reference signal) is introduced to compute a characteristic time scale. However, both self-excited oscillation and resonance frequencies generally correspond to natural system frequencies, and dimensionless models should include them in order to portray the system's magnitude orders in the right way. Within this discussion, a systematic approach both for computing this characteristic time scale and for computing characteristic measures of the dependent variables is proposed. The resulting dimensionless system equations clearly reveal two different magnitude orders, which motivates the utilization of an asymptotic method. The system is represented as a singularly perturbed third-order differential equation. Herein, the valve's main nonlinearity, which is its non-smooth flow characteristic, is not small. This nonlinearity must be accounted for in the zero-order solution of the asymptotic approximation. By means of singular perturbation and averaging techniques, a first-order approximation of the slow mani-
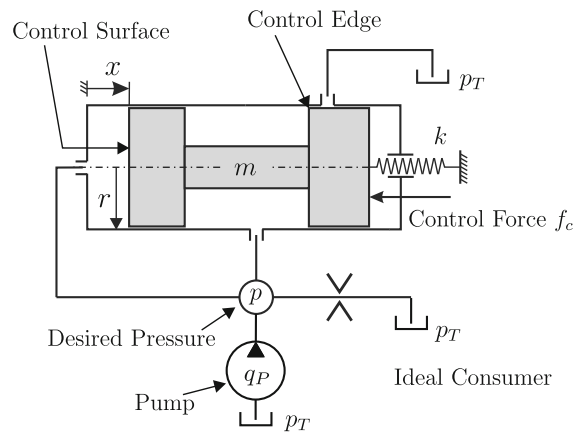

Fig. 1 Hydraulic circuit under investigation including pump, pressure control valve and consumer

fold is derived and approximate solutions for the self-excited oscillations of the valve are computed. The procedure is then extended, so that also forced vibrations, evoked by pump pulsations, can be approximated. The results are validated by comparison with full timescale numerical simulations.

2 Pressure control valve model

This section presents a simple hydraulic circuit, which is used for the investigation of pressure control valve dynamics. First, a physical representation is derived, followed by a dimensional analysis of dependent and independent variables. Based upon this analysis, a dimensionless model of the circuit is presented.

2.1 Physical system representation

The hydraulic circuit investigated in this paper is depicted in Fig. 1. The principal components of the system are a pump, an ideal consumer and the valve itself. The consumer is modeled as a simple hydraulic resistance. Following the usual modeling approaches for the investigation of stability and dynamics of hydraulic systems [12,16,27], the governing equations are given by

$$m\ddot{x} + d\dot{x} + kx = r^2\pi p - f_c, \tag{1}$$
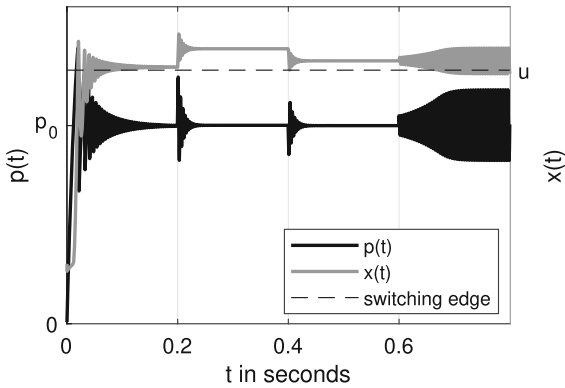$$C_h\dot{p} = q_P - r^2\pi\dot{x} + q_h(x, p). \tag{2}$$

Fig. 2 Transient system behavior and self-excited oscillations. Initial conditions are $x(0) = 0$m, $\dot{x}(0) = 0$ms^{-1}, $p(0) = 0$bar

Herein, parameters m, k and r denote mass, stiffness and radius of the valve piston and the control force f_c represents either a spring preload, a solenoid force or a static pressure force applied by a pilot stage. Spool position x and pressure p represent the dependent variables. Parameters q_P and C_h are the constant pump volume flow and system's hydraulic capacitance and the function q_h, representing the system's nonlinear flow characteristic including non-smooth control edge flow and nonlinear volume flow to consumer, reads

$$q_h(x, p) = -\gamma_V (\sigma(x - u)2r\pi(x - u) + A_C)\Delta(p - p_T),$$

with γ_V the turbulent flow coefficient, u the valve overlap, A_C the area of the orifice representing the ideal consumer and with $\sigma(x)$ and $\Delta(p)$ defined as

$$\sigma(x) = \begin{cases} 1, & x \geq 0 \\ 0, & x < 0 \end{cases}, \quad \Delta(p) = \begin{cases} \sqrt{p}, & p \geq 0 \\ -\sqrt{|p|}, & p < 0 \end{cases}.$$

Expression $d\dot{x}$ can be seen as a surrogate for various frictional effects in the system. Secondary physical effects such as hydraulic inductance, Bernoulli forces, position-dependent capacitance and Coulomb friction are not taken into consideration.

The working principle of the valve is demonstrated in Fig. 2, showing numerical simulations of the transient responses of spool position $x(t)$ and system pressure $p(t)$ to a change in consumer demand (change of orifice area A_C) at $t = 0.2$ s and in power supply (change of pump volume flow q_P) at $t = 0.4$ s. As expected, stationary system pressure p_0 is maintained, whereas the stationary spool position x_0 varies

depending on the difference between supply and load volume flow. Through enlargement of spool mass m at $t = 0.6$ s, the valve's equilibrium position is destabilized and limit cycle oscillations emerge. Here, Piston oscillation amplitudes are approximately 0.15 mm and pressure amplitudes are about 5.5 bar, which are rather high values. This is due to the fact that the simulation involves a high pump volume flow of $q_P = 20$ l/m. The simulations are carried out with the parameter ranges given in Table 1, whose values are orientated on real valves. All numerical simulations are computed with Matlab, using its ode23t-solver including event-detection of the switching edge.

2.2 Scaling of dependent and independent variables

In order to find the "right" scaling for a non-dimensional system representation, it is noted that the parameter values, with which the numerical simulations of the limit cycle oscillations in Fig. 2 at $t > t_3$ are performed, are chosen so that the valve is operated in an unstable parameter domain, but close to the stability border. It strikes that the piston oscillations $x(t)$ crosses the switching edge, but only to a small extent. As a matter of fact, further numerical simulations show that this is always the case in proximity to the stability border. Hence, under the assumption that the piston oscillates approximately symmetrical around its equilibrium position, the distance $x_0 - u$ between equilibrium position $x = x_0$ of valve spool and switching edge $x = u$ seems to be a characteristic distance measure, at least in proximity to the bifurcation point, which is also the parameter domain of the most practical interest.

For the computation of this measure, it is shown in the sequel how to derive approximations for the stationary valve position x_0 and, as a by-product, set-pressure p_0. Along with $p_T = 0$Pa, the equilibrium conditions of Eqs. (1) and (2) read

$$kx_0 = r^2\pi p_0 - f_c, \tag{3}$$

$$0 = q_P - \gamma_V (2r\pi(x_0 - u) + A_C)\sqrt{p_0}. \tag{4}$$

At this point, it is useful to assume that $kx_0 \ll f_c$. This is a typical case and is always strived for in pressure control valve design, because it corresponds to a precise preservation of the set-pressure level p_0, as can be directly seen from Eq. (3). Following this assumption, the approximate stationary equilibrium

Table 1 Parameter values used for the numerical simulations. In case a range is given, underlined represent the standard values

Parameter	Symbol	Value	Unit
Spool mass	m	$\underline{0.018}\ldots0.072$	kg
Damping coeff.	d	$\underline{180}\ldots240$	N s/m
Spring stiffness	k	2000	N/m
Control force	f_c	150	N
Spool radius	r	0.004	m
Valve overlap	u	0.002	m
Pump flow	q_P	$\underline{5}\ldots20$	l /min
Orifice area	A_C	$(\underline{1}\ldots5)\cdot\pi\cdot(10^{-3})^2$	m^2
Capacitance	C_h	$4.17\cdot10^{-13}$	m^3/Pa
Flow coefficient	γ_V	0.03	$\sqrt{\text{m}^3/\text{kg}}$

$$\tilde{p}_0 = \frac{f_c}{r^2\pi}, \quad \tilde{x}_0 = u + \frac{q_P}{2r\pi\gamma_V}\sqrt{\frac{r^2\pi}{f_c}} - \frac{A_C}{2r\pi} \quad (5)$$

takes a relatively simple form. The parameters in Table 1 correspond to a stationary set-pressure level $\tilde{p}_0 \approx 30$bar. For the exact computation of the equilibrium position, the reader is referred to [16] or [27].

A characteristic time scale can be found by assuming that the piston inertia is small compared to pressure and damping forces, which is also a rather typical case [14]. Neglecting it in Eq. (1) allows to express the system pressure and its time derivative as

$$p = \frac{1}{r^2\pi}(d\dot{x} + kx + f_c), \quad \dot{p} = \frac{1}{r^2\pi}(d\ddot{x} + k\dot{x}).$$

Along with Eq. (2) and by performing a Taylor series expansion of the nonlinear volume flow function q_h around the approximate equilibrium position, the representation of a linear damped oscillator

$$\frac{C_h}{r^2\pi}(d\ddot{x} + k\dot{x}) = q_P - r^2\pi\dot{x} + q_h(x,p)$$

$$\approx q_p - r^2\pi\dot{x} + q_h(\tilde{x}_0,\tilde{p}_0) + \left.\frac{\partial q_h}{\partial x}\right|_{\tilde{x}_0,\tilde{p}_0}(x - \tilde{x}_0)$$

$$+ \left.\frac{\partial q_h}{\partial p}\right|_{\tilde{x}_0,\tilde{p}_0}\left(\frac{1}{r^2\pi}(d\dot{x} + kx + f_c) - \tilde{p}_0\right)$$

is derived, whose approximate (considering, that $k \ll \left.\frac{\partial q_h}{\partial x}\right|_{\tilde{x}_0,\tilde{p}_0}$) undamped angular frequency

$$\omega^2 = \left.\frac{\partial q_h}{\partial x}\right|_{\tilde{x}_0,\tilde{p}_0}\left(\frac{C_h d}{r^2\pi}\right)^{-1} = \frac{2r\pi\,\gamma_V}{C_h\,d}\sqrt{r^2\pi\,f_c} \quad (6)$$

is a natural choice for the introduction of a characteristic time scale. With standard parameter values given in Table 1, a characteristic angular frequency of $\omega \approx 934$rad/s is obtained. For the parameters of the limit cycle oscillations in Fig. 2, a value of $\omega \approx 810$rad/s is computed, which is an acceptable rough estimation for the actual oscillation angular frequency of ≈ 730rad/s.

2.3 Dimensionless system representation

The non-dimensional variables and parameters

$$\tau = \omega t, \ X = \frac{x - u}{\tilde{x}_0 - u}, \ P = \frac{p\,r^2\pi}{d\,\omega\,\tilde{x}_0}, \ M = \frac{m\omega}{d},$$

$$\alpha_1 = \frac{(r^2\pi)^2}{\omega d C_h}, \ F_c = \frac{ku + f_c}{d\omega\tilde{x}_0}, \ \alpha_V = \sqrt{\frac{r^2\pi\tilde{x}_0}{\omega^3 d}}\frac{2r\pi\gamma_V}{C_h},$$

$$K = \frac{k}{d\omega}, \ \alpha_C = \sqrt{\frac{r^2\pi}{\omega^3 d\tilde{x}_0}}\frac{A_C\gamma_V}{C_h}, \ Q_P = \frac{r^2\pi q_P}{\omega^2\tilde{x}_0 dC_h}$$

are introduced by using the characteristic quantities from Eqs. (5) and (6). This leads to the piecewise smooth (continuous, but not continuously differentiable) non-dimensional system representation

$$MX'' + X' + KX = P - F_c, \quad (7)$$

$$P' = Q_P - \alpha_1 X' + Q_h(X, P). \quad (8)$$

Parameters M, K and F_c are the dimensionless spool mass, spring stiffness and control force and Q_P and

Table 2 Two sets of dimensionless parameter values. The set used in Sect. 3 is computed with standard values from Table 1. The other one is computed with an increased damping of $d = 240$ Ns/ m

Dimensionless parameter	Symbol	Value (Sect. 3)	Value (Sect. 4)
Spool mass	M	0.093	0.061
Spring stiffness	K	0.012	0.010
Control force	F_c	27.98	24.23
Pump flow	Q_P	1.955	1.955
Control surface	α_1	0.036	0.031
Spool diameter	α_V	0.192	0.206
Orifice area	α_C	0.183	0.197

α_1 are the dimensionless pump volume flow and control surface. Superscript primes denote derivatives with respect to the dimensionless time τ. The dimensionless volume flow characteristic of the valve reads

$$Q_h(X, P) = - \begin{cases} (\alpha_V X + \alpha_C)\sqrt{P}, & X > 0 \\ \alpha_C \sqrt{P}, & X \le 0 \end{cases} \quad (9)$$

with α_V and α_C the dimensionless spool diameter and orifice area.

The values of the newly introduced dimensionless parameters are given in Table 2. With values in the third column, the valve's equilibrium position is unstable; it is therefore used in Sect. 3. Parameter values in the fourth column lead to a stable equilibrium position, and the simulation results in Sect. 4 are carried out with them.

3 Approximate solutions of self-excited oscillations

Within this section, the procedure for computing asymptotic approximations for the limit cycle amplitude and frequency of the pressure control valve model is described. The procedure combines classical singular perturbation with an averaging technique, as suggested, for example, in [28]. This procedure is closely related to the asymptotic analysis of partially damped systems proposed in [6] and generalized in [5]. Firstly, the system is reformulated as a third-order ordinary differential equation, which, as it appears, is singularly perturbed. Secondly, the singularly perturbed (fast) variable is approximated with an asymptotic expansion up to magnitude order ε. This approximation converts the singularly perturbed system into a regularly perturbed one, on which first-order averaging is applied.

3.1 Asymptotic approximation of the slow manifold

In order to clarify the magnitude orders, the new variable $\xi = X - X_0$, representing deviations from the equilibrium position, is introduced and Eqs. (7) and (8) are reformulated as a single ordinary differential equation of third order

$$M\xi''' + \xi'' + K\xi' = Q_P - \alpha_1\xi'$$
$$+ Q_h(\xi + X_0, M\xi'' + \xi' + K\xi + P_0), \quad (10)$$

in which $P_0 = K X_0 + F_c$ is the dimensionless stationary set-pressure. With the parameters given in Table 1, the dimensionless mass is small, i.e., $M \ll 1$. Therefore, Eq. (10) is a singularly perturbed equation. The usual procedure in handling such equations is to separate slow variables ξ, ξ' and the fast variable $\eta = \xi''$, cf. [4,28]. Furthermore, to enable the application of asymptotic methods, Taylor series expansions of the two switching states of the nonlinear volume flow characteristic Q_h, Eq. (9), are executed around the equilibrium position $[\xi, \xi', \xi'']^\top = [0, 0, 0]^\top$. By introducing a small parameter $\varepsilon = M$ and neglecting terms of magnitude order ε^2 and higher, one obtains the piecewise smooth system representation

$$\xi'' = \eta, \quad (11)$$
$$\varepsilon\eta' = -\eta + \begin{cases} -\varepsilon K_o\xi' - \omega_o^2\xi - \varepsilon N_o\xi'\xi, & \xi + X_0 > 0 \\ -\varepsilon K_c\xi' + Q_c, & \xi + X_0 \le 0 \end{cases},$$
$$=: g(\xi, \eta, \varepsilon), \quad (12)$$

in which all newly introduced parameters

$$K_o = \frac{K + \alpha_1 + \beta_o}{\varepsilon}, \quad \omega_o^2 = \alpha_V \sqrt{P_0} + K\beta_o,$$

Table 3 Two sets of dimensionless parameter values for the system representation defined by Eqs. (11) and (12). The two sets based on the same physical parameter values as the sets in Table 2

Symbol	Value (Sect. 3)	Value (Sect. 4)
K_o	0.89	1.35
K_c	0.70	1.01
ω_o	1.01	1.01
Q_c	0.99	0.99
N_o	0.19	0.34

$$N_o = -\frac{K\beta_o}{2P_0\varepsilon} + \frac{\alpha_V}{2\sqrt{P_0}\varepsilon},$$

$$K_c = \frac{K + \alpha_1 + \beta_c}{\varepsilon}, \quad Q_c = Q_P - \sqrt{P_0}\alpha_C,$$

are of magnitude order one, see Table 3.

In fact, parameter value N_o is at least significantly higher than magnitude order ε and therefore considered as magnitude order 1. Parameters

$$\beta_o = \frac{\alpha_V X_0 + \alpha_C}{2\sqrt{P_0}}, \quad \beta_c = \frac{\alpha_C}{2\sqrt{P_0}}$$

stem from the Taylor series expansions of the two switching states of Q_h. The expressions $\varepsilon\eta'$ and $\varepsilon K_i \xi'$, $i = \{o, c\}$, associated with inertia and spring forces, are of magnitude order ε, which is in agreement with the assumptions stated in Sect. 2.2. The subscripts $\{o, c\}$ are associated with the two switching states indicating whether the valve is open ($\xi + X_0 > 0$) or closed ($\xi + X_0 \leq 0$). It is noted that the exact same system representation as in Eqs. (11) and (12) with the same magnitude orders can be derived for valves with pressure supply instead of volume flow supply, as studied in [12–14], but only if the magnitude orders of the difference between supply pressure and system pressure match the magnitude order of the system pressure itself.

In terms of singular perturbation theory, an asymptotic approximation for the limit cycle oscillations corresponds to a regular or outer expansion of the solution [28]. For autonomous systems, this outer expansion can be associated with a so-called slow manifold $\mathcal{M}_\varepsilon$ in phase space. By setting $\varepsilon = 0$ in the boundary layer Eq. (12), a continuous but non-smooth first-order approximation $\mathcal{M}_0$ of the slow manifold $\mathcal{M}_\varepsilon$
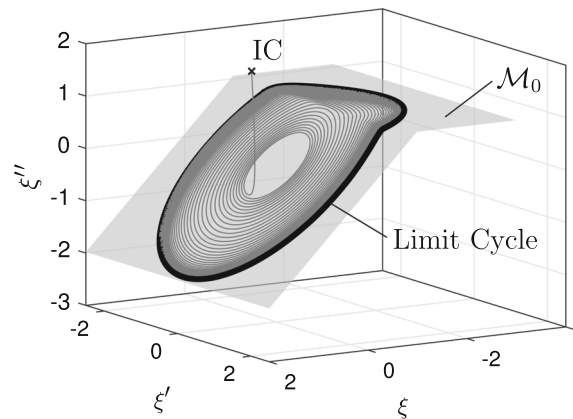

Fig. 3 Three-dimensional phase space containing first-order approximation $\mathcal{M}_0$ of the slow manifold and numerically simulated trajectory of the full system Eq. (10). Initial conditions indicated as IC

$$\eta = \begin{cases} -\omega_o^2 \xi, & \xi + X_0 > 0 \\ Q_c, & \xi + X_0 \leq 0 \end{cases}, \tag{13}$$

is obtained. This is a globally asymptotically stable (eigenvalue -1) solution of the equation

$$\frac{d\eta}{d\theta} = g(\xi, \eta, 0),$$

in which ξ is a parameter and not a variable. Hence, all solutions of Eqs. (11) and (12) are attracted by the slow manifold.

Figure 3 shows the three-dimensional phase space of the full system, in which the first-order approximation of the slow manifold $\mathcal{M}_0$ is represented as a light gray, bent surface. One can clearly see that the trajectory, starting at the point indicated as IC, is strongly attracted by it and remains in an ε-vicinity for all time.

3.2 Asymptotic approximation of the system dynamics on the slow manifold

The flow on the slow manifold is described by Eq. (11). Herein, the fast variable η appears with magnitude order one, why an asymptotic expansion $\eta \approx \tilde{\eta} = \eta_0 + \varepsilon\eta_1$ up to magnitude order ε has to be computed first. Substituting it into Eq. (12) and balancing terms with the same magnitude orders, the asymptotic approximation up to magnitude order ε can be directly computed to

$$\tilde{\eta} = \begin{cases} -\omega_o^2 \xi + \varepsilon((\omega_o^2 - K_o)\xi' - N_o\xi'\xi), & \xi + X_0 > 0 \\ Q_c - \varepsilon K_c\xi', & \xi + X_0 \leq 0 \end{cases}$$

$$(14)$$

by solving linear algebraic equations. It is noted that this approximation, in contrast to Eq. (13), is not continuous at $\xi = -X_0$ anymore. By substituting Eq. (14) into Eq. (11), the singularly perturbed system, Eqs. (11) and (12), is transformed into the regularly perturbed equation

$$\xi'' = \begin{cases} -\omega_o^2 \xi + \varepsilon((\omega_o^2 - K_o)\xi' - N_o\xi'\xi), & \xi + X_0 > 0 \\ Q_c - \varepsilon K_c\xi', & \xi + X_0 \leq 0 \end{cases},$$

$$(15)$$

describing the flow on the slow manifold, on which averaging [24] is applied subsequently.

Substituting the asymptotic expansions $\xi \approx \tilde{\xi} = \xi_0 + \varepsilon\xi_1, \xi' \approx \tilde{\xi}' = \xi_0' + \varepsilon\xi_1'$ into Eq. (15) and balancing terms with magnitude order ε^0 delivers the zero-order solutions

$$\xi_0(\tau) = \begin{cases} \xi_0^o(\tau) = A\cos(\omega_o\tau + \alpha), & \tau_0 < \tau \leq \tau_1 \\ \xi_0^c(\tau) = c_1 + c_2\tau + \frac{1}{2}Q_c\tau^2, & \tau_1 < \tau \leq \tau_2 \end{cases}$$

$$(16)$$

$$\xi_0'(\tau) = \begin{cases} \xi_0^{o'}(\tau) = -A\omega_o\sin(\omega_o\tau + \alpha), & \tau_0 < \tau \leq \tau_1 \\ \xi_0^{c'}(\tau) = c_2 + Q_c\tau, & \tau_1 < \tau \leq \tau_2 \end{cases}$$

$$(17)$$

of the slow variables with integration constants A, α, c_1 and c_2. The constants c_1 and c_2 as well as the unknown switching times τ_0, τ_1 and τ_2 can be expressed in dependence of A and α by solving transition conditions

$$\xi_0^o(\tau_0) = -X_0, \ \xi_0^o(\tau_1) = -X_0, \ \xi_0^{o'}(\tau_1) = \xi_0^{c'}(\tau_1),$$

$$(18)$$

$$\xi_0^c(\tau_1) = -X_0, \ \xi_0^c(\tau_2) = -X_0,$$

$$(19)$$

cf. Fig. 4.

Note that the zero-order solution $\xi_0(\tau)$ is continuously differentiable also at $\tau = \tau_2$, although this condition is not explicitly formulated. Solving the above conditions gives expressions

$$\tau_0 = \frac{-\alpha - \pi + C}{\omega_o}, \ \tau_1 = \frac{-\alpha + \pi - C}{\omega_o},$$

$$\tau_2 = \tau_1 + \frac{2\omega_o}{Q_c}\sqrt{A^2 - X_0^2}, \ c_2 = -Q_c\tau_1 - \omega_o\sqrt{A^2 - X_0^2},$$
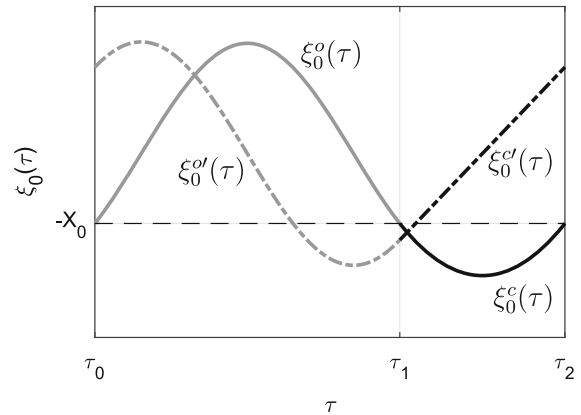
Fig. 4 Structure of zero-order solutions $\xi_0(\tau)$ and $\xi_0'(\tau)$ with according switching times, $A = 1.5$
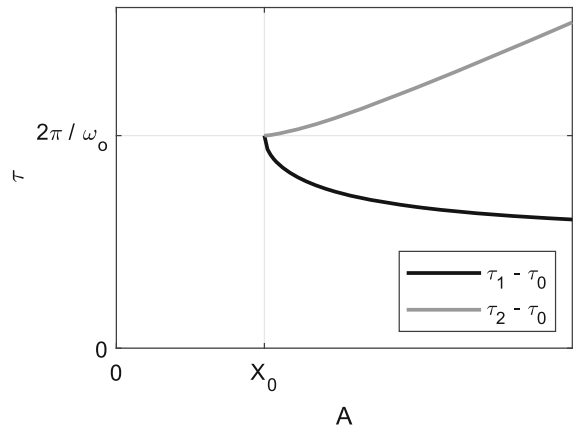

Fig. 5 Switching times in dependence of amplitude A

$$c_1 = \frac{1}{2}\tau_1^2 Q_c + (\pi - \alpha - C)\sqrt{A^2 - X_0^2} - X_0,$$

$$C = \arccos\left(\frac{X_0}{A}\right)$$

in dependence of A and α only, see Fig. 5.

A system in standard form for averaging can be obtained by varying constants $A = A(\tau)$ and $\alpha = \alpha(\tau)$ and using Eqs. (16) and (17) as a variable transformation with $\xi = \xi_0, \xi' = \xi_0'$. Inserting this transformation into Eq. (15), a non-smooth system of differential equations in the form

$$A' = \varepsilon \begin{cases} f_{A_o}(\tau - i\Delta\tau), & \tau_0 + i\Delta\tau \leq \tau < \tau_1 + i\Delta\tau \\ f_{A_c}(\tau - i\Delta\tau), & \tau_1 + i\Delta\tau \leq \tau < \tau_2 + i\Delta\tau \end{cases}$$

$$(20)$$

$$\alpha' = \varepsilon \begin{cases} f_{\alpha_o}(\tau - i\Delta\tau), & \tau_0 + i\Delta\tau \le \tau < \tau_1 + i\Delta\tau \\ f_{\alpha_c}(\tau - i\Delta\tau), & \tau_1 + i\Delta\tau \le \tau < \tau_2 + i\Delta\tau \end{cases}$$

$$\Delta\tau = \tau_2 - \tau_0, \quad i = 0, 1, 2, \ldots \quad (21)$$

for the variables A and α with right hand sides of magnitude order ε is derived. It is subsequently averaged

$$A' = \frac{\varepsilon}{\tau_2 - \tau_0} \left(\int_{\tau_0}^{\tau_1} f_{A_o}(\tau)\mathrm{d}\tau + \int_{\tau_1}^{\tau_2} f_{A_c}(\tau)\mathrm{d}\tau \right)$$

$$= -\varepsilon \left(6A(\omega_o^2\sqrt{A^2 - X_0^2} + Q_c(\pi - \mathcal{C})) \right)^{-1}$$

$$\times \left(\left(2(N_0 Q_c + K_c \omega_o^2)(A^2 - X_0^2) \right. \right.$$

$$+ 3X_0 Q_c (K_o - \omega_o^2) \Big)$$

$$\times \left. \sqrt{A^2 - X_0^2} - 3A^2 Q_c(\omega_o^2 - K_o)(\pi - \mathcal{C}) \right) \quad (22)$$

with respect to dimensionless time τ providing a smooth right hand side. Variable $A(\tau)$ represents the maxima of the limit cycle oscillations. The corresponding minima

$$A_{\min}(\tau) = \xi_0^c(\tau = 1/2(\tau_1 + \tau_2))$$

$$= \frac{1}{2}\frac{\omega_o^2}{Q_c}(X_0^2 - A^2) - X_0$$

are computed along with Eq. (16). The dimensionless oscillation frequency can be computed from $f = (\tau_2 - \tau_0)^{-1}$, which does not depend on variable α. Therefore, the relevant equation for variable α is of no interest. The computation of the steady-state amplitude can be performed very efficiently numerically, either by calculating the root of the right hand side or by numerical time integration of Eq. (22). So far, extensive parameter studies have not yielded coexisting or unstable solutions corresponding to periodic solutions of the full system. This is an important result of practical interest, meaning that attraction domains of stable equilibrium solutions of the original system are not limited by unstable limit cycles. The existence condition for the solution of Eq. (22) results from the argument of $\mathcal{C} = \arccos(X_0/A)$, namely $A > X_0$. That means that Eq. (22) is only valid for oscillations crossing the switching edge.

In case of oscillations not crossing the switching edge, $A < X_0$, the averaging takes the form

$$A' = \varepsilon \frac{\omega_o}{2\pi} \int_0^{\frac{2\pi}{\omega_o}} f_{A_o}(\tau)\mathrm{d}\tau = -\frac{\varepsilon}{2}(K_o - \omega_o^2)A. \quad (23)$$

As a by-product of this result, the stability condition

$$K_o - \omega_o^2 < 0$$

for the equilibrium position of the valve, corresponding to a stable trivial solution $A = 0$ of Eq. (23), can directly be computed, which with the dimensionless parameters from Sect. 3.1 and upon simplifying assumptions $P_0 \approx F_c$, $X_0 \approx 1$ and $K \ll 1 < F$ leads to

$$-(K + \alpha_1)\sqrt{F_c} + \alpha_V \left(MF_c - \frac{1}{2} \right) - \frac{1}{2}\alpha_C < 0.$$

An increase of spring stiffness K or a decrease of the slope of the flow characteristic, corresponding to dimensionless parameter α_V, stabilizes the equilibrium position, which is in accordance with the results presented in [16] and [13].

Because the right hand side of Eq. (20) is not continuous, the classical proofs for the validity of the asymptotic approximations do not hold here; however, they are validated by comparison with full time numerical simulations, see Fig. 6. Both the transient decay and the steady-state amplitude are reproduced excellently. Figure 7 shows a comparison between dimensionless oscillation frequencies f computed from original and averaged equations under variation of the small parameter $\varepsilon = M$. The results show a reasonable concordance, even for relatively high values of the small parameter ε. The same holds true for the oscillation minima and maxima, see Fig. 8. With these results, the question of what the limitations of the proposed method are, can be addressed. These are related to the small parameter ε. As an example, it is assumed that for $\varepsilon < 0.2$ the approximation is within an allowable error margin. In regard to the allowable physical parameters, e.g., system damping—starting from the standard values in Table 1—can be reduced to $d \approx 100\,\mathrm{N\,s/m}$, or the hydraulic capacitance can be reduced to $C_h \approx 10^{-13}\,\mathrm{m}^3/\mathrm{Pa}$ without the method failing.
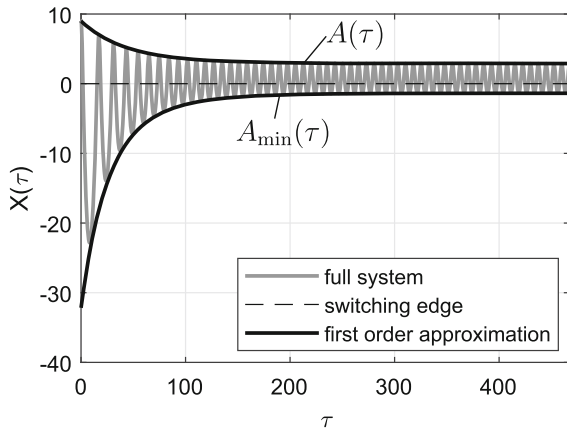
Fig. 6 Comparison between numerical solutions of full system and averaged equation. The simulation corresponds to $t = 0.5\,\mathrm{s}$ in the original time scale. The corresponding physical steady-state oscillation amplitudes of the piston are approximately 0.05 mm, which leads to pressure oscillation amplitudes of about 1.5 bar
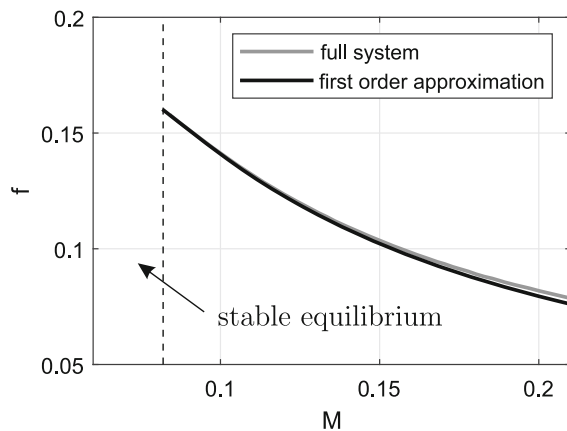

Fig. 7 Comparison between non-dimensional stationary oscillation frequency f calculated from full system and averaged equation

4 Approximate solutions of forced oscillations

Apart from self-excited vibrations, another important scenario of practical interest in connection with nonlinear valve dynamics is the case of a valve being operated under stable conditions, but subject to periodic excitation. In real-world applications, these excitation can be evoked from pump pulsations, unstable neighboring valves or a dithering signal. It is expected that forced oscillation amplitudes remain not small in case of a resonant excitation, meaning that the excitation frequency matches the valve's natural frequency ω.
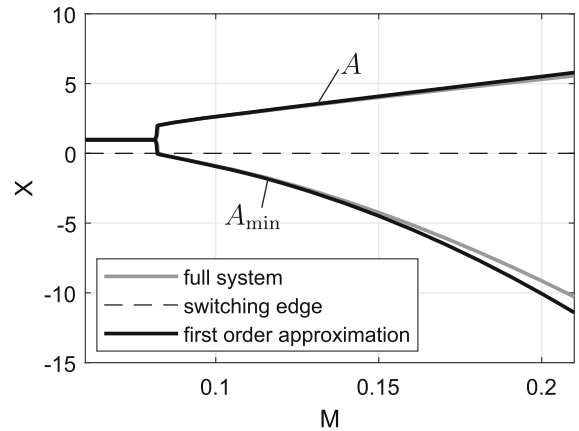

Fig. 8 Comparison between non-dimensional stationary oscillation minima $A_{\min}$ and maxima A calculated from full system and averaged equation

The above described procedure can easily be modified in order to obtain asymptotic approximations of the system response to a harmonic excitation. The case of pump pulsations is considered here. For this case, the non-dimensional pump volume flow is assumed to be of the form

$$Q_P = Q_P(\tau) = Q_{P0} + \varepsilon A_Q \cos(\Omega_Q \tau),$$

in which parameter A_Q is assumed to be of magnitude order one. Hence, the excitation amplitude is of magnitude order ε. Following the procedure described in Sect. 3, the governing equation for the slow variables, Eq. (15), takes the form

$$\xi'' = \begin{cases} -\omega_o^2 \xi + \varepsilon((\omega_o^2 - K_o)\xi' - N_o \xi' \xi), & \xi + X_0 > 0 \\ Q_c + \varepsilon - K_c \xi', & \xi + X_0 \leq 0 \end{cases}$$
$$+ \varepsilon A_Q \cos(\Omega_Q \tau). \tag{24}$$

It is noteworthy that in the present case it would be possible not to approximate the stationary solution of the fast dynamics by a series approach, but to compute it directly. This can be done by introducing the so-called strongly damped variable $y = \eta - \eta_0$ (compare [5]). Through this transformation, all expressions containing slow variables ξ, ξ' are of magnitude order ε, which is why they can be seen as constant in this case. Since the equation of the fast dynamics is linear in η (and y, respectively), it can be explicitly solved. In this exact solution, the harmonic excitation would

cause an additional phase shift, which is, however, of magnitude order ε^2. As expected, numerical simulations have shown for the present case that this does not result in a significant improvement of the approximate solution.

It is clear that the zero-order solutions of the slow variables, Eqs. (16) and (17), must be modified to ensure that the period of the zero-order solution matches the excitation period. There are several modification possibilities, and one has to keep in mind that the analytical manipulations necessary for the later averaging procedure must remain possible. From here on, it is assumed that the excitation frequency is nearby the resonance frequency; that means $|\Omega_Q - \omega_o| \ll 1$. To keep the equations as simple as possible, the zero-order solutions

$$\xi_0(\tau) = \begin{cases} \xi_0^o(\tau) = A\cos(\Omega_Q\tau + \psi), & \tau_0 < \tau \le \tau_1 \\ \xi_0^c(\tau) = c_1 + c_2\tau + \frac{1}{2}Q_c\kappa\tau^2, & \tau_1 < \tau \le \tau_2 \end{cases}$$

$$\xi_0'(\tau) = \begin{cases} \xi_0^{o'}(\tau) = -A\Omega_Q\sin(\Omega_Q\tau + \psi), & \tau_0 < \tau \le \tau_1 \\ \xi_0^{c'}(\tau) = c_2 + Q_c\kappa\tau, & \tau_1 < \tau \le \tau_2 \end{cases}$$

are proposed with phase variable ψ. Parameter κ has to be computed so that the period of the zero-order solution matches the period of the excitation. Solving the same conditions as in (18) and (19) but with $\tau_2 - \tau_0 = 2\pi/\Omega_Q$, expressions

$$\tau_0 = \frac{-\psi - \pi + \mathcal{C}}{\Omega_Q}, \quad \tau_1 = \frac{-\psi + \pi - \mathcal{C}}{\Omega_Q},$$

$$\kappa = \frac{\Omega_Q^2(2A + X_0)}{3Q_c}, \quad \mathcal{C} = \arccos\left(\frac{X_0}{A}\right),$$

$$c_2 = -\frac{1}{3}(2A + X_0)\Omega_Q^2\tau_1 - \Omega_Q\sqrt{A^2 - X_0^2},$$

$$c_1 = \frac{1}{6}(2A + X_0)\Omega_Q^2\tau_1^2 + \Omega_Q\tau_1\sqrt{A^2 - X_0^2} - X_0$$

are derived. The further procedure is identical to that of the autonomous case, except that the cosine term in Eq. (24) for $\xi + X_0 < 0$ has to be approximated by a quadratic polynomial, which is computed by a Taylor series expansion around $\tau = (\tau_0 + 2\pi/\Omega_Q + \tau_1)/2$. This approximation is done in order to enable the analytical computation of the averaged equations, which are, however, too lengthy to write them here.

The numerical simulations in Fig. 9 are executed with a stable parameter set with increased damping compared to that used in the previous section, see
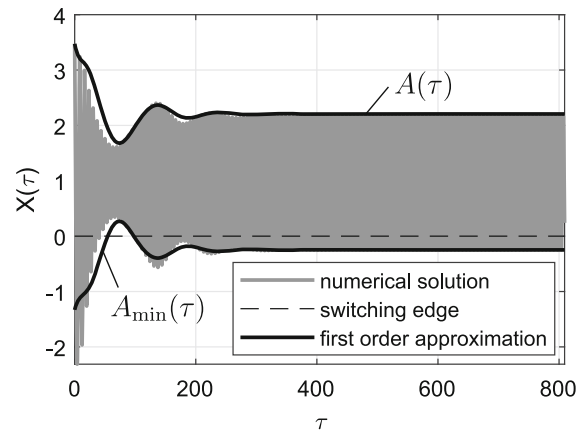

Fig. 9 Comparison between numerical solutions of full system and averaged equation, $\Omega_Q = 1$, $A_Q = 1$. The simulation corresponds to $t = 1$ s in the original time scale

Tables 2 and 3. The transient system behaviors of full system and first-order approximation are in good agreement, at least qualitatively.

According to Fig. 10, also the stationary maxima and minima of the forced vibrations show a reasonable concordance. Stationary solution curves for $A < X_0$ even lie almost on top of each other, so that no difference is visible. Larger deviations can be seen for the case $A > X_0$ in proximity to the highest resonance peak. In particular, the first-order approximation underestimates the region, in which multiple solutions exist. The dashed lines correspond to unstable solutions, which most likely also exist in the full system, but are not computed here.

5 Conclusions

Within this contribution, the nonlinear dynamics of a hydraulic pressure control valve have been investigated by means of asymptotic approximations. After introducing the hydraulic circuit including pump, control valve and ideal consumer, the working principle has been demonstrated by numerical simulations of the transient system behavior, showing that the stationary set-pressure is maintained independently of the power supply and consumer demand. It has also been shown that the valve's internal feedback loop can cause stability problems and the occurrence of limit cycle oscillations.
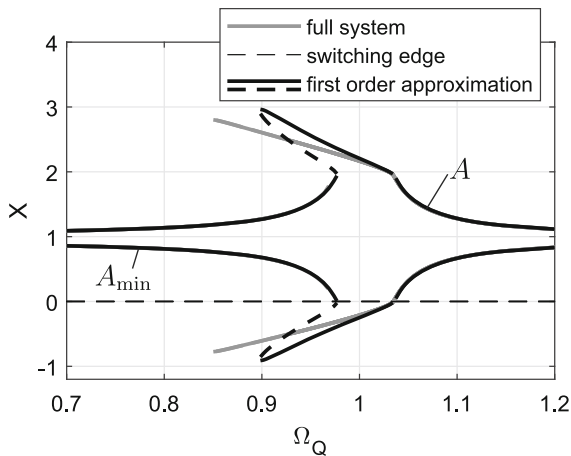
Fig. 10 Nonlinear amplitude response. Comparison between stationary solutions of full system and averaged equation, $A_Q = 1$. Dashed lines correspond to unstable periodic solutions

In order to prepare asymptotic analysis, considerations with regard to magnitude orders of system parameters and states have clarified that pressure and damping forces dominate inertia and spring forces. By neglecting the non-dominant forces, simple expressions for the equilibrium position and a characteristic system frequency have been derived, which are suitable for the scaling of dependent and independent variables of the system.

Because of the consideration of a very light piston, the dimensionless system representation is a singularly perturbed third-order differential equation. It has been shown that the limit cycle oscillations can be associated with a slow manifold in phase space, whose attraction properties have been demonstrated numerically and theoretically, the latter by showing that the corresponding first order approximation is a globally asymptotically stable solution of the unperturbed equation of the fast variable. The singularly perturbed problem has been transformed into a regularly perturbed equation by computing asymptotic approximations of the fast variable up to magnitude order ε.

The scaling considerations have also revealed that the switching nonlinearity of the valve's control edge flow is not small. Consequently, to capture the system's dominant nonlinearity, a non-smooth zero-order solution of the slow variable has been constructed, which subsequently has been used as a variable transformation to obtain a system in standard form for averaging. With this procedure, the non-smooth third-order system

representation has been reduced to a first-order differential equation. The asymptotic approximations have been validated by comparison with numerical simulations of the original system equations and have shown to give a good estimate of limit cycle oscillation amplitude and frequency.

For the approximation of the forced system response due to pump pulsations, the zero-order solution of the slow variable has been modified in order to match its period and that of the excitation. The analytical expressions obtained from averaging are more complex; however, both transient and stationary solutions are well represented.

Compliance with ethical standards

References

1. Bazsó, C., Hös, C.J.: An experimental study on the stability of a direct spring loaded poppet relief valve. J. Fluids Struct. **42**, 456–465 (2013). https://doi.org/10.1016/j.jfluidstructs.2013.08.008
2. Dankowicz, H., Fotsch, E.: On the analysis of chatter in mechanical systems with impacts. Procedia IUTAM **20**, 18–25 (2017). https://doi.org/10.1016/j.piutam.2017.03.004
3. Eyres, R.D., Piiroinen, P.T., Champneys, A.R., Lieven, N.A.J.: Grazing bifurcations and chaos in the dynamics of a hydraulic damper with relief valves. SIAM J. Appl. Dynam. Syst. **4**(4), 1076–1106 (2005). https://doi.org/10.1137/040619697
4. Fenichel, N.: Geometric singular perturbation theory for ordinary differential equations. J. Differ. Equ. **31**(1), 53–98 (1979). https://doi.org/10.1016/0022-0396(79)90152-9
5. Fidlin, A., Drozdetskaya, O.: On the averaging in strongly damped systems: The general approach and its application

to asymptotic analysis of the sommerfeld effect. Procedia IUTAM **19**, 43–52 (2016). https://doi.org/10.1016/j.piutam.2016.03.008

6. Fidlin, A., Thomsen, J.J.: Non-trivial effects of high-frequency excitation for strongly damped mechanical systems. Int. J. Non-Linear Mech. **43**(7), 569–578 (2008). https://doi.org/10.1016/j.ijnonlinmec.2008.02.002

7. Funk, J.E.: Poppet valve stability. J. Basic Eng. **86**(2), 207–212 (1964). https://doi.org/10.1115/1.3653036

8. Hayashi, S.: Instability of poppet valve circuit. JSME Int. J. Ser. C , Dynamics, Control, Robotics, Design and Manuf. **38**(3), 357–366 (1995). https://doi.org/10.1299/jsmec1993.38.357

9. Hayashi, S., Hayase, T., Kurahashi, T.: Chaos in a hydraulic control valve. J. Fluids Struct. **11**(6), 693–716 (1997). https://doi.org/10.1006/jfls.1997.0096

10. Hös, C.J., Champneys, A.R.: Grazing bifurcations and chatter in a pressure relief valve model. Physica D **241**(22), 2068–2076 (2012). https://doi.org/10.1016/j.physd.2011.05.013

11. Köster, M.: On modeling, analysis and nonlinear control of hydraulic systems. Ph.D. thesis, Karlsruhe Institute of Technology, Karlsruhe (2017). https://doi.org/10.5445/IR/1000070929

12. Köster, M., Fidlin, A.: Nonlinear dynamics of a hydraulic pressure control valve. Proceedings of the 11th International Conference on Vibrating Problems (2013)

13. Kremer, E.: About absolute stability of control valves. 6th EUROMECH Nonlinear Dynamics Conference (ENOC 2008) (2008)

14. Kremer, E.: Slow motions in systems with fast modulated excitation. J. Sound Vib. **383**, 295–308 (2016). https://doi.org/10.1016/j.jsv.2016.07.006

15. Kremer, E.: Low-frequency response of controlled systems on a high-frequency parametric excitation. ENOC **2017**, (2017)

16. Licskó, G., Champneys, A.R., Hös, C.J.: Nonlinear analysis of a single stage pressure relief valve. IAENG Int. J. Appl. Math. **39**(12), (2009)

17. Lin, C.C., Segel, L.A.: Mathematics Applied to Deterministic Problems in the Natural Sciences. Macmillan, New York (1974)

18. Lucente, G., Montanari, M., Rossi, C.: Modelling of an automated manual transmission system. Mechatronics **17**(2–3), 73–91 (2007). https://doi.org/10.1016/j.mechatronics.2006.11.002

19. Ma, C.Y.: The analysis and design of hydraulic pressure-reducing valves. J. Eng. Indus. **89**(2), 301–308 (1967). https://doi.org/10.1115/1.3610044

20. Maccari, A.: Saddle-node bifurcations of cycles in a relief valve. Nonlinear Dyn. **22**, 225–247 (2000). https://doi.org/10.1023/A:1008349500673

21. Manhartsgruber, B.: Application of singular perturbation theory to hydraulic servo drives-system analysis and control design. In: Proceedings of the 1st FPNI PhD Symposium Hamburg pp. 339–352 (2000)

22. Manhartsgruber, B., Scheidl, R.: Nonlinear control of hydraulic servo drives based on a singular perturbation approach. Bath Workshop on Power Transmission and Motion Control (1998). https://doi.org/10.13140/RG.2.1.3048.2000

23. Nayfeh, A.H., Bouguerra, H.: Non-linear response of a fluid valve. Int. J. Non-Linear Mech. **25**(4), 433–449 (1990). https://doi.org/10.1016/0020-7462(90)90031-4

24. Sanders, J.A., Murdock, J., Verhulst, F.: Averaging Methods in Nonlinear Dynamical Systems, Applied Mathematical Sciences, vol. 59. Springer, New York (2007). https://doi.org/10.1007/978-0-387-48918-6

25. Scheidl, R., Manhartsgruber, B.: On the dynamic behavior of servo-hydraulic drives. Nonlinear Dyn. **17**, 247–268 (1998). https://doi.org/10.1023/A:1008348714791

26. Schröders, S., Fidlin, A.: Oscillations in a system of two coupled self–regulating spool valves with switching properties. Proc. Appl. Math. Mech. (PAMM) 19(1) (2019). https://doi.org/10.1002/pamm.201900340

27. Schröders, S., Fidlin, A.: Analyse des dynamischen verhaltens zweier gekoppelter druckregelventile. Forsch. Ingenieurwes. **84**(2), 205–213 (2020). https://doi.org/10.1007/s10010-020-00401-6

28. Verhulst, F.: Methods and applications of singular perturbations: Boundary layers and multiple timescale dynamics, Texts in applied mathematics, vol. 60. Springer, New York (2005). https://doi.org/10.1007/0-387-28313-7